nists (LY367385 and scopolamine) or the vehicle bilaterally into the dorsal EC and subjected these mice to TFC. In response to tone, the freezing level of antagonist-injected control mice was less than vehicle-injected control mice, but was not different from antagonist-injected mutants (Fig. 4F). With the same pharmacological treatment, we observed no freezing difference to tone between the genotypes in the DFC task (fig. S16)

In this study, we created a transgenic mouse line in which the synaptic output of the excitatory MEC layer III cells is specifically and reversibly inhibited. Our genetic manipulation and behavior data provided insights into the specific role of MEC layer III projection in the processing of hippocampal-dependent memory.

First, the MECIII input to the HP, an essential component of the MSP, is crucial for temporal associations in spatial working memory. The DMP task required animals to update the association between the platform location and spatial cues daily on the first run and maintain that association for subsequent runs that same day. The DNMP task required animals to associate the sample arm and the alternative reward arm across a delay period. Both of these tasks require a temporal association memory with a temporal gap of 15 to 30 s. Although it is possible that the deficits observed in the mutants are due to their inability to encode spatial/contextual information, this is unlikely because these animals were normal in other spatial/contextual memory tasks (figs. S12 to 14 and S17). Second, a blockade of the MECIII input into the HP resulted in an impairment in TFC, specifically during day 1 when the animals needed to associate the CS and US delivered with an intervening 20-s gap. Again, it is unlikely that the deficits are due to an inability to encode the CS or US because the same mutants were normal in DFC and even in a TFC task with a 40-s trace that may not be hippocampal-dependent (fig. S18) (*21*). Third, our demonstration that the alternative and indirect input to CA1 mediated by the TSP is dispensable for TFC highlights the importance of the MSP in temporal association memory.

In addition to the major projections to CA1/subiculum, MECIII neurons send axons to other EC cells (*22*). We expect that these connections

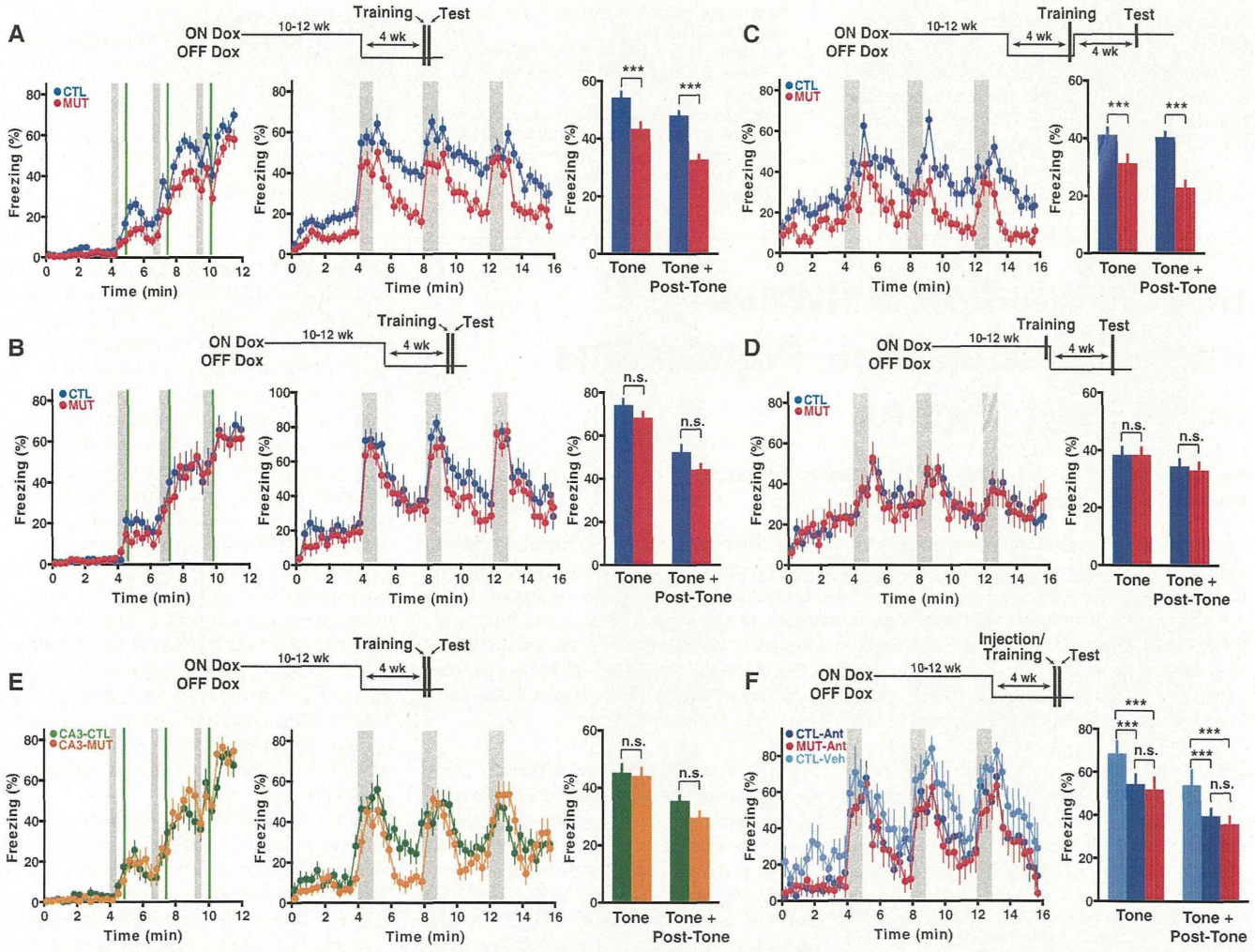

Fig. 4. Fear conditionings with two mutants, MECIII-TeTX and CA3-TeTX, and pharmacologically treated mice. (**A** and **B**) Time course of freezing observed in MECIII-TeTX mice in the TFC (A) or DFC task (B) during training on day 1 (left) and testing on day 2 (middle). Gray and green bars represent tone and shock, respectively. Freezing levels during the testing were averaged over three epochs of the 60-s tone period and of the entire 240-s tone plus post-tone periods (right). (**C** and **D**) Time course of freezing (left) and averaged freezing levels (right) of MECIII-TeTX mice during testing of the TFC task in which the synaptic inhibition was targeted to the training (C) or testing (D). (**E**) Time course of freezing of CA3-TeTX mice during the training (left) and testing (middle) of the TFC task. (**F**) Time course of freezing (left) and averaged freezing levels (right) during testing for controls and mutants in the TFC task. Mice were bilaterally injected with either an antagonist mixture or vehicle into dorsal MEC before the training. Asterisks indicate the significance at the level of 0.05 or less; error bars indicate SEMs. n.s., not significant.

are also blocked in the mutants and therefore cannot exclude the possibility that an impairment of intrinsic ECIII circuits contributed to the observed behavioral deficits. However, such an impairment alone can not explain the observed deficits in the hippocampal-dependent memory tasks unless it is translated into an MSP impairment. Thus, a more attractive possibility would be that the lack of transmission of persistent activity from the MECIII (*19*) to CA1/subiculum via the MSP resulted in the behavioral deficits in these hippocampal-dependent tasks, although such activity has yet to be demonstrated in vivo in the mouse. We hypothesize that tone induces sustained activity in the MECIII after its cessation. This persistent activity, perhaps with the help of theta and/or gamma frequency coupling between the MECIII and CA1 (and/or subiculum) (*23*, *24*), may allow the delivery of the CS to the amygdala through CA1 (and/or subiculum) in a manner coincidental with the US signal. The differential effects of the mGluR1 and cholinergic muscarinic receptor antagonists injected into MEC on the TFC and DFC tasks (Fig. 4F and fig. S16) support this hypothesis.

Apart from specific mechanisms, our overall results demonstrate a crucial role of the EC layer III input to the HP in hippocampal-dependent temporal association memory.

References and Notes

1. M. E. Hasselmo, C. E. Stern, *Trends Cogn. Sci.* **10**, 487 (2006).
2. A. Baddeley, *Nat. Rev. Neurosci.* **4**, 829 (2003).
3. N. S. Clayton, T. J. Bussey, A. Dickinson, *Nat. Rev. Neurosci.* **4**, 685 (2003).
4. T. J. McHugh *et al.*, *Science* **317**, 94 (2007).
5. T. Nakashiba, J. Z. Young, T. J. McHugh, D. L. Buhl, S. Tonegawa, *Science* **319**, 1260 (2008).
6. K. Nakazawa *et al.*, *Science* **297**, 211 (2002).
7. K. Nakazawa, T. J. McHugh, M. A. Wilson, S. Tonegawa, *Nat. Rev. Neurosci.* **5**, 361 (2004).
8. R. P. Kesner, P. E. Gilbert, G. V. Wallenstein, *Curr. Opin. Neurobiol.* **10**, 260 (2000).
9. D. G. Mumby, *Behav. Brain Res.* **127**, 159 (2001).
10. H. A. Steffenach, M. Witter, M. B. Moser, E. I. Moser, *Neuron* **45**, 301 (2005).
11. V. H. Brun *et al.*, *Science* **296**, 2243 (2002).
12. Materials and methods are available as supporting material on *Science* Online.
13. M. P. Witter, D. G. Amaral, in *The Rat Nervous System*, G. Paxinos, Ed. (Elsevier Academic Press, New York, 2004), pp. 635–704.
14. T. Tominaga, Y. Tominaga, H. Yamada, G. Matsumoto, M. Ichikawa, *J. Neurosci. Methods* **102**, 11 (2000).
15. Relevant discussion regarding data in figs. S12 and S14 can be found in the supporting online material.
16. K. Nakazawa *et al.*, *Neuron* **38**, 305 (2003).
17. R. J. Steele, R. G. Morris, *Hippocampus* **9**, 118 (1999).
18. A. V. Egorov, B. N. Hamam, E. Fransén, M. E. Hasselmo, A. A. Alonso, *Nature* **420**, 173 (2002).
19. M. Yoshida, E. Fransén, M. E. Hasselmo, *Eur. J. Neurosci.* **28**, 1116 (2008).
20. F. Esclassan, E. Coutureau, G. Di Scala, A. R. Marchand, *J. Neurosci.* **29**, 8087 (2009).
21. I. Misane *et al.*, *Hippocampus* **15**, 418 (2005).
22. C. B. Canto, F. G. Wouterlood, M. P. Witter, *Neural Plast.* **2008**, 1 (2008).
23. K. Mizuseki, A. Sirota, E. Pastalkova, G. Buzsáki, *Neuron* **64**, 267 (2009).
24. L. L. Colgin *et al.*, *Nature* **462**, 353 (2009).

Acknowledgments: We thank C. Ragion, C. Twiss, M. Pfau, M. Ragion, C. Carr, and S. Perry for technical help; N. Arzoumanian for help with manuscript preparation; and D. Buh, J. Young, and other members of the Tonegawa lab for discussion. This work was supported by NIH grants R01-MH078821 and P50-MH58880 (to S.T.) and the RIKEN Brain Science Institute.

Supporting Online Material

www.sciencemag.org/cgi/content/full/science.1210125/DC1
Materials and Methods
SOM Text
Figs. S1 to S18
References

21 June 2011; accepted 20 October 2011
Published online 3 November 2011;
10.1126/science.1210125

Interconversion Between Intestinal Stem Cell Populations in Distinct Niches

Norifumi Takeda,[1,2,3]* Rajan Jain,[1,2,3]* Matthew R. LeBoeuf,[1,4] Qiaohong Wang,[1,2,3] Min Min Lu,[2] Jonathan A. Epstein[1,2,3]†

Intestinal epithelial stem cell identity and location have been the subject of substantial research. Cells in the +4 niche are slow-cycling and label-retaining, whereas a different stem cell niche located at the crypt base is occupied by crypt base columnar (CBC) cells. CBCs are distinct from +4 cells, and the relationship between them is unknown, though both give rise to all intestinal epithelial lineages. We demonstrate that *Hopx*, an atypical homeobox protein, is a specific marker of +4 cells. *Hopx*-expressing cells give rise to CBCs and all mature intestinal epithelial lineages. Conversely, CBCs can give rise to +4 *Hopx*-positive cells. These findings demonstrate a bidirectional lineage relationship between active and quiescent stem cells in their niches.

The multicellular epithelium of the intestine is replaced every few days, and this renewal process is maintained by multipotent intestinal stem cells (ISCs) (*1*, *2*). The location and identity of ISCs have been a subject of much research and debate, with implications for understanding gastrointestinal cancer, repair after intestinal injury, and normal physiology. Numerous reports have suggested that ISCs are located at the +4 position relative to the crypt base (*3*, *4*), while a separate body of work has identified a distinct stem cell niche at the crypt base where crypt base columnar (CBC) cells are interspersed between Paneth cells (*5*–*7*). The +4 cells correspond to the location of slow-cycling, label-retaining cells (LRCs) (*3*, *8*) and colocalize with *Bmi1*-expressing cells (*4*), as well as those expressing an *mTert* transgene (*9*, *10*). CBC stem cells, by contrast, are marked by *Lgr5* (*5*). Although +4 cells and CBCs are clearly distinct, lineage-tracing studies have shown that both can give rise to all the various cell types comprising the small intestine epithelium: goblet cells, neuroendocrine cells, Paneth cells, and epithelial absorptive cells. However, the relationship between these two distinct stem cell populations remains incompletely understood. A recent report suggests that +4 cells can compensate for the loss of CBCs to maintain homeostasis after experimental ablation of *Lgr5*-expressing cells (*11*). However, a bidirectional lineage relationship between active and quiescent populations of stem cells in multiple tissues has also been postulated (*2*), though experimental evidence to support this proposal has been lacking. Here, we show that quiescent +4 ISCs express the atypical homeobox gene *Hopx* and give rise to *Lgr5*-expressing CBCs. Conversely, rapidly cycling CBCs expressing *Lgr5* give rise to +4 cells expressing *Hopx*. These findings reconcile controversies regarding the location and identity of ISCs and demonstrate interconversion between organ-specific stem cell niches.

Hopx encodes an atypical homeodomain-containing protein that has previously been studied in the heart and neural stem cells (*12*–*14*). Analysis of the intestines of *Hopx lacZ* knock-in ($Hopx^{LacZ/+}$) mice revealed robust expression of β-galactosidase (β-Gal) in intestinal crypts along the entire length of the intestine (Fig. 1A and fig. S1A). Expression was strongest in the +4 region and included label-retaining cells identified after irradiation and pulse labeling with 5-bromodeoxyuridine (BrdU) (*9*, *15*, *16*) (Fig. 1B and fig. S1B). Eighty-six percent (68/79) of non-Paneth BrdU-retaining cells expressed β-Gal, and nearly all were at or near the +4 position

[1]Department of Cell and Developmental Biology, Perelman School of Medicine at the University of Pennsylvania, Philadelphia, PA 19104, USA. [2]Penn Cardiovascular Institute, Perelman School of Medicine at the University of Pennsylvania, Philadelphia, PA 19104, USA. [3]Institute of Regenerative Medicine, Perelman School of Medicine at the University of Pennsylvania, Philadelphia, PA 19104, USA. [4]Department of Dermatology, Perelman School of Medicine at the University of Pennsylvania, Philadelphia, PA 19104, USA.

*These authors contributed equally to this work.
†To whom correspondence should be addressed. E-mail: epsteinj@mail.med.upenn.edu

J_ID: STEM Customer A_ID: STEM1083 Date: 16-March-12 Stage: Page: 1

STEM CELLS®

REGENERATIVE MEDICINE

Treatment of a Mouse Model of Spinal Cord Injury by Transplantation of Human Induced Pluripotent Stem Cell-Derived Long-Term Self-Renewing Neuroepithelial-Like Stem Cells

YUSUKE FUJIMOTO,[a,b] MASAHIKO ABEMATSU,[b] ANNA FALK,[c] KEITA TSUJIMURA,[a] TSUKASA SANOSAKA,[a] BERRY JULIANDI,[a,d] KATSUNORI SEMI,[a] MASAKAZU NAMIHIRA,[a] SETSURO KOMIYA,[b] AUSTIN SMITH,[c] KINICHI NAKASHIMA[a]

[a]Laboratory of Molecular Neuroscience, Graduate School of Biological Sciences, Nara Institute of Science and Technology, Ikoma, Japan; [b]Department of Orthopaedic Surgery, Graduate School of Medical and Dental Sciences, Kagoshima University, Kagoshima, Japan; [c]Department of Biochemistry, Wellcome Trust Centre for Stem Cell Research, University of Cambridge, Cambridge, United Kingdom; [d]Department of Biology, Bogor Agricultural University (IPB), Bogor, Indonesia

Key Words. Spinal cord injury • Induced pluripotent stem cells • Neural stem cells • Transplantation • Regenerative medicine

ABSTRACT

Because of their ability to self-renew, to differentiate into multiple lineages, and to migrate toward a damaged site, neural stem cells (NSCs), which can be derived from various sources such as fetal tissues and embryonic stem cells, are currently considered to be promising components of cell replacement strategies aimed at treating injuries of the central nervous system, including the spinal cord. Despite their efficiency in promoting functional recovery, these NSCs are not homogeneous and possess variable characteristics depending on their derivation protocols. The advent of induced pluripotent stem (iPS) cells has provided new prospects for regenerative medicine. We have recently developed a robust and stable protocol for the generation of long-term, self-renewing, neuroepithelial-like stem cells from human iPS cells (hiPS-lt-NES cells), which can provide a homogeneous and well-defined population of NSCs for standardized analysis. Here, we show that transplanted hiPS-lt-NES cells differentiate into neural lineages in the mouse model of spinal cord injury (SCI) and promote functional recovery of hind limb motor function. Furthermore, using two different neuronal tracers and ablation of the transplanted cells, we revealed that transplanted hiPS-lt-NES cell-derived neurons, together with the surviving endogenous neurons, contributed to restored motor function. Both types of neurons reconstructed the corticospinal tract by forming synaptic connections and integrating neuronal circuits. Our findings indicate that hiPS-lt-NES transplantation represents a promising avenue for effective cell-based treatment of SCI. STEM CELLS *2012; 000: 000–000*

Disclosure of potential conflicts of interest is found at the end of this article.

INTRODUCTION

Our current ability to reconstruct the damaged central nervous system, including spinal cord injury (SCI), is limited. SCI is one of the commonest causes of loss of movement and sensation below the level of the injured spinal cord. While partial spontaneous functional recovery has been observed in the case of moderate SCI, there is no adequate treatment to repair the injured spinal cord itself, and most patients have no therapeutic options except for general management and rehabilitation [1].

Transplantation of neural stem cells (NSCs) into the injured spinal cord has been shown to be an effective treatment [2] because of their competence to differentiate into neurons and oligodendrocytes and to secrete neurotrophic factors. Transplantation into injured spinal cords of several different types of human NS/progenitor cells, derived from human fetal tissue [3, 4] or from human embryonic stem cells (hESCs) [5, 6], promotes functional recovery in animal models. Nonetheless, the mechanism underlying such functional improvement remains to be fully elucidated.

The establishment of induced pluripotent stem cells (iPSCs) offers new prospects for regenerative therapies [7, 8]. Human iPSCs (hiPSCs) can be generated from cells in adult tissue, making it possible to create iPSCs from SCI patients themselves. From the viewpoint of ethics and host immune rejection, NSCs derived from human iPSCs (hiPS-NSCs)

Author contributions: Y.F.: conception and design, collection and assembly of data, data analysis and interpretation, and manuscript writing; A.F. and A.S.: provision of study materials; M.A., K.T., T.S., K.S., and M.N.: collection and assembly of data, data analysis and interpretation; B.J.: manuscript writing; S.K.: administrative support; K.N.: conception and design, administrative support, manuscript writing, and final approval of manuscript.

Correspondence: Kinichi Nakashima, Ph.D., Laboratory of Molecular Neuroscience, Graduate School of Biological Sciences, Nara Institute of Science and Technology, 8916-5 Takayama, Ikoma 631-0192, Japan. Telephone: 81-743-72-5471; Fax: 81-743-72-5479; e-mail: kin@bs.naist.jp. Received October 18, 2011; accepted for publication February 11, 2012; first published online in STEM CELLS *EXPRESS* Month 00, 2012. 1066-5099/2012/$30.00/0 doi: 10.1002/stem.1083

ID: ananda | Black Lining: [ON] | Time: 11:31 | Path: N:/3b2/STEM/Vol00000/120053/APPFile/JW-STEM120053

appear to be an ideal resource for transplantation therapy, and the efficacy of hiPS-NSC transplantation in SCI treatment has just begun to be investigated using the mouse model of SCI [9].

We have recently developed a protocol for the generation of long-term self-renewing neuroepithelial-like stem (lt-NES) cells, which satisfy the criteria to be defined as NSCs, from several different lines of hESCs and hiPSCs [10, 11]. hiPSC-derived lt-NES (hiPS-lt-NES) cells exhibit consistent characteristics such as continuous expandability, stable neuronal and glial differentiation ability, and the capacity to generate functional mature neurons in monolayer culture. Whereas neurosphere cultures display heterogeneous character and are sensitive to variation in methodological procedures [12], monolayer cultures offer a more homogeneous and robust cell generation [13, 14].

We report here that transplanted hiPS-lt-NES cells, derived from our robust and stable monolayer cultures, have a therapeutic potential comparable to that of NSCs from human fetal spinal cord (hsp-NSCs) for SCI in the nonobese diabetic-severe combined immunodeficient (NOD-SCID) mouse model. We further show that hiPS-lt-NES cell transplantation promotes recovery of hind limb motor function through the reconstruction of the corticospinal tract (CST), and restores disrupted neuronal circuitry in a relay manner as we have previously demonstrated in a study of mouse NSC transplantation [15]. Our results suggest that hiPS-lt-NES cells represent a promising cell source for transplantation into the injured spinal cord.

Materials and Methods

Cell Culture

hsp-NSCs and hiPS-lt-NES cells were established and maintained as described previously [10, 11, 16]. The hsp-NS cell line CB660sp and hiPS-lt-NES cell line AF22 were used in the present study. hsp-NSCs were plated onto 10 μg/ml laminin (Sigma, St. Louis, MO, http://www.sigmaaldrich.com)-coated plates in maintenance medium, consisting of Euromed-N medium (Euroclone, Milano, Italy, http://www.euroclonegroup.it), 2 mM L-glutamine, 0.1 mg/ml penicillin/streptomycin (Sigma), N2 supplement (1:100), 20 ml/l B27 (all from Invitrogen, Carlsbad, CA, http://www.invitrogen.com), 10 ng/ml fibroblast growth factor (FGF, R&D Systems, Minneapolis, MN, http://www.rndsystems.com)-2, and 10 ng/ml epidermal growth factor (EGF, R&D Systems). Cells were passaged at a ratio of 1:2 every second to third day using Accutase (Sigma). hiPS-lt-NES cells were plated onto 0.1 mg/ml poly-L-ornithine and 10 μg/ml laminin (O/L, Sigma)-coated plates in maintenance medium, consisting of Dulbecco's modified Eagle's medium/F12 (Invitrogen), 2 mM L-glutamine, 1.6 mg/ml glucose, 0.1 mg/ml penicillin/streptomycin, N2 supplement (1:100), 1 μl/ml B27, 10 ng/ml FGF2 and 10 ng/ml EGF. Cells were passaged at a ratio of 1:3 every second to third day using trypsin. To induce in vitro differentiation, hiPS-lt-NES cells were plated onto an O/L-coated 35-mm dish at a density of 5×10^5 cells per dish in culture medium without both EGF and FGF, containing 1% fetal bovine serum (FBS), and cultured for 4 weeks. Half of the medium was changed every 2 days and laminin (1:500) was added to the medium once a week to prevent detachment of the cells.

Lentivirus Production and Infection of hsp-NSCs and hiPS-Lt-NES Cells

Lentivirus production and infection of cells were performed as described previously [17, 18]. hsp-NSCs and hiPS-lt-NES cells were infected with lentiviruses harboring the luciferase and green fluorescent protein (GFP) genes connected by an internal ribosomal entry site (IRES), EFp (elongation factor promoter)-luciferase-IRES-GFP (Fig. 1B). hsp-NSCs and hiPS-lt-NES cells that had undergone more than 20 passages were infected. GFP-positive cells were collected by fluorescence activated cell sorting (FACS)-Aria II CellSorter (B.D. Biosciences, San Jose, CA, http://www.bdbiosciences.com) and used for transplantation. F1

SCI Model and Cell Transplantation

All aspects of animal care and treatment were carried out according to the guidelines of the experimental animal care committee of Nara Institute of Science and Technology. We used female NOD-SCID mice (8-10 weeks old, weighing 18-20 g, Charles River, Osaka, Japan, http://www.crj.co.jp). Anesthetized (ketamine 50 mg/kg, xylazine 5 mg/kg, and sodium pentobarbital 20 mg/kg) mice received laminectomies and partial laminectomies at the ninth and 10th thoracic spinal vertebrae, respectively. The dorsal surface of the dura mater was exposed and SCI was induced using an SCI device (70 kdyn; Infinite Horizon impactor, Precision Systems & Instrumentation, Lexington, KY, http://www.presysin.com) as previously described [15]. The muscle and skin were closed in layers. All mice subcutaneously received gentamicin (8 mg/kg) daily. The mice underwent manual bladder evacuation once a day. Seven days after injury, mice were anesthetized and transplanted with hiPS-lt-NES cells or hsp-NSCs using a glass micropipette attached to a stereotaxic injector (Narishige, Tokyo, Japan, http://www.narishige.co.jp). The tip of the micropipette was inserted into the injury epicenter in the injured spinal cord, and 2 μl of culture medium lacking growth factors, with or without NSCs (5×10^5 μl^{-1}), was injected at a rate of 1 μl/min.

Behavioral Testing and Electrophysiological Recordings

We evaluated the motor function of the hind limbs for up to 10 weeks after injury. Two individuals, blinded to the treatment of the mice, examined motor function using the Basso Mouse Scale (BMS) locomotor rating scale [19]. Hind limb movements of the mice were captured using a high-definition digital camcorder. We edited these movies and exported movie files using editing software.

To examine signal conduction in motor pathways after SCI, motor-evoked potentials (MEPs) at 12 weeks after SCI were measured. Mice were anesthetized with intraperitoneally injected ketamine (100 mg/kg) and their heads were fixed in a stereotactic frame. The skulls were tightly fixed to a stereotaxic apparatus (Narishige). Scalping and two small craniotomies were performed with a drill over the motor cortex area (Nakanishi, Tochigi, Japan; http://www.nsk-nakanishi.co.jp). Silver ball electrodes were placed epidurally via the holes, into which mineral oil was applied. The motor cortex was stimulated with 0.2-msecond square wave pulses at a constant current of 10 mA using an electrical stimulator (SEM-3301, Nihon Kohden, Tokyo, Japan; http://www.nihonkohden.co.jp). Recording needle electrodes were inserted into the hamstring. A subcutaneous ground electrode was placed in the tail. Electrophysiological recordings were made (MED64, Alpha MED Scientific, Osaka, Japan; http://www.amedsci.com) and band-pass filtered at 1-10 kHz. Amplitudes from onset to peak of the negative deflection were measured. Latency of MEP was measured as the time interval between the end of stimulation and the onset of the first wave. Indicated values are the average of five experiments from each mouse.

Antibodies

The following antibodies were used: rabbit anti-Sox2 (1:1,000, Chemicon-Millipore, Billerica, MA, http://www.millipore.com), mouse anti-Nestin (1:250, Chemicon), rabbit anti-brain lipid-binding protein (BLBP, 1:500, Abcam, Cambridge, U.K., http://www.abcam.com), mouse anti-β-tubulin isotype III (Tuj1; 1:500,

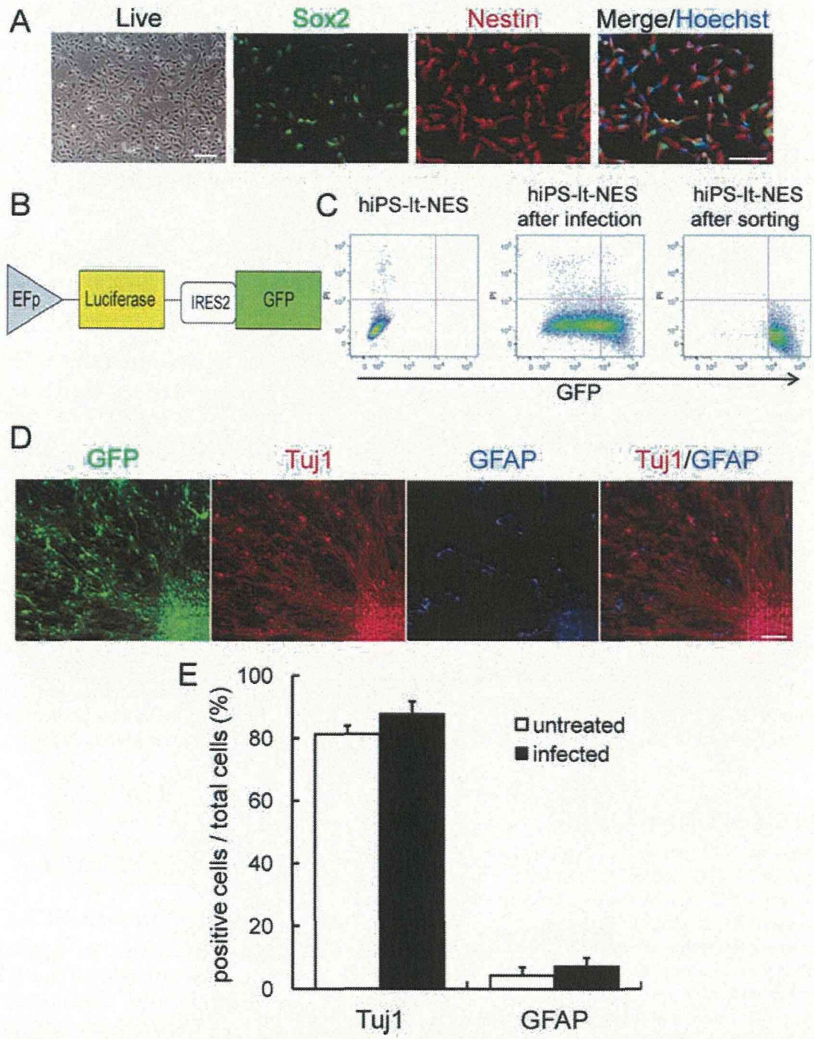

COLOR

Figure 1. Characterization of hiPS-lt-NES cells. **(A):** Expansion culture. hiPS-lt-NES cells can be expanded continuously in the presence of both epidermal growth factor and fibroblast growth factor. hiPS-lt-NES cells were uniformly immunopositive for Sox2 (green) and Nestin (red). Hoechst (blue) shows nuclear staining. **(B):** The pCSII-EFp-luciferase-IRES2-GFP construct. **(C):** Flow cytometric analysis of GFP-positive cells in hiPS-lt-NES cells. Uninfected cells (left) and cells infected with lentiviruses expressing luciferase and GFP (middle) were subjected to flow cytometric analysis. GFP-positive cells in the infected cell population were sorted on the basis of GFP fluorescence and reanalyzed for GFP expression (right). **(D):** After 4 weeks in differentiation conditions, infected hiPS-lt-NES cells differentiated into Tuj1-positive neurons (red) and GFAP-positive astrocytes (blue). **(E):** Quantification of neural marker-positive cells after 4 weeks' differentiation. Lentiviral infection did not influence the differentiation tendency. Data are means ± SD ($n = 3$). Scale bars = 100 μm. Abbreviations: EFp, elongation factor promoter; GFP, green fluorescent protein; GFAP, glial fibrillary acidic protein; hiPS-lt-NES, human induced pluripotent stem cell-derived long-term self-renewing neuroepithelial-like stem; and IRES2, internal ribosomal entry site 2.

Sigma), rabbit anti-β-tubulin isotype III (Tuj1; 1:1,000, Covance, Madison, WI, http://www.covance.com), rabbit anti-GFP (1:1,000, Molecular Probes, Carlsbad, CA, http://probes.invitrogen.com), chick anti-GFP (1:500, Aves Labs, Tigard, OR, http://www.aveslab.com), rabbit anti-glial fibrillary acidic protein (GFAP, 1:2,000, DAKO, Carpinteria, CA, http://www.dako.com), mouse anti-human-specific GFAP (hGFAP, 1:1,000, STEM123, StemCells Science, Newark, CA, http://www.stemcellsinc.com), mouse anti-MAP2ab (1:500, Sigma), chick anti-MBP (1:200, Aves Labs), mouse anti-adenomatous polyposis coli CC-1 (APC, 1:200, Calbiochem-Merck, Darmstadt, Germany, http://www.merckgroup.com), mouse anti-synaptophysin (1:200, Chemicon), mouse anti-Bassoon (Bsn, 1:400, Stressgen-Enzo Life Sciences, Plymouth Meeting, PA, http://www.enzolifesciences.com), mouse anti-human-specific synaptophysin (hSyn, 1:200, Chemicon), and mouse anti-NeuN (1:500, Millipore).

Immunocytochemistry

Immunocytochemistry experiments were performed as described previously [20]. Cells were washed with phosphate buffered saline (PBS) and fixed with 4% paraformaldehyde (PFA) in PBS for 10 minutes, and then washed with PBS and incubated in blocking solution (PBS containing 10% FBS and 0.1% Triton X-100). Subsequently, cells were incubated overnight at 4°C with the primary antibodies described above. After three washes in PBS, cells were incubated for 1 hour with the following secondary antibodies: FITC-conjugated donkey anti-chick/rabbit, Cy3-

conjugated donkey anti-chick/mouse/rabbit, Cy5-conjugated donkey anti-mouse/rabbit (1:500, Jackson ImmunoResearch, West Grove, PA, http://www.jacksonimmuno.com). After three washes with PBS, nuclei were stained with Hoechst (bisbenzimide H33258 fluorochrome trihydrochloride, Calbiochem-Merck). Samples were washed with PBS and mounted on glass slides with Immu-Mount (Thermo Scientific, Waltham, MA, http://www.thermoscientific.com). The cells were examined using a fluorescence microscope (Axiovert 200M, Zeiss, Jena, Germany, http://www.zeiss.com) equipped with the appropriate epifluorescence filters.

Immunohistochemistry

Animals were anesthetized and perfused with PBS followed by 4% PFA in 0.1 M PBS, pH 7.4. The spinal cords were dissected and postfixed overnight in the same fixative at 4°C. For cryosectioning, fixed tissues were cryoprotected in 10% sucrose in PBS overnight at 4°C, then in 20% sucrose in PBS overnight at 4°C, and embedded in OCT compound (Tissue Tek, Sakura Finetek, Tokyo, Japan, http://www.sakura-finetek.com). Cryostat sections (20 μm) were cut and affixed to MAS-coated glass slides (Matsunami Glass, Osaka, Japan, http://www.matsunami-glass.co.jp). The sections were permeabilized in PBS-T (PBS containing 0.1% Triton X-100) for 10 minutes and blocked with 10% FBS in PBS-T for 1 hour, and then incubated overnight at 4°C with the primary antibodies described above. After three washes with PBS, they were incubated in a mixture of the secondary antibodies described above for 1 hour. After a final rinse with PBS, nuclei were stained using Hoechst. Sections were mounted and examined under a fluorescence microscope (Axiovert 200M, Zeiss) and a scanning laser confocal imaging system (LSM 710, Zeiss).

In Vivo Imaging of Transplanted Cells

In vivo imaging experiments were performed as described previously [18]. A Xenogen-IVIS 100 cooled CCD optical macroscopic imaging system (SC BioScience, Tokyo, Japan, www.scbio.co.jp) was used for bioluminescence imaging. Mice were given an intraperitoneal injection of D-luciferin (150 mg/kg) and serial images were acquired from 20 minutes after administration until the maximum intensity was obtained with the field-of-view set at 10 cm. All images were analyzed using Igor (WaveMetrics, Portland, OR, http://www.wavemetrics.com) and Xenogen Living Image software, and optical signal intensity was expressed as photon flux in units of photons/s per cm^2/steradian. To quantify the measured light, we defined regions of interest (ROIs) over the cell-implanted area and examined all values within the same ROI. The obtained photon count intensity was expressed as a percentage of the initial value.

Anterograde Labeling of the CST

Twelve weeks after injury, descending CST fibers were labeled with biotinylated dextran amine (BDA) (MW 10,000, 10% in saline, 2 μl per cortex; Molecular Probes) [21, 22] by injection into the left and right motor cortices [23]. The skulls of anesthetized mice were tightly fixed to a stereotaxic apparatus (Narishige). Scalping and craniotomy over the motor cortex area were carried out using a micromotor system (Nakanishi). The injection site was 2.1 mm posterior to the bregma, 2 mm lateral to the bregma, and 0.7 mm in depth [23]. For pressure injections with a 20-μm outer diameter glass capillary attached to a microsyringe (Narishige), we used 0.1-μl steps per minute until the desired volume (1 μl per injection site) was injected. Two weeks later, the animals were perfused and their spinal cords were fixed as described above. Sections (30 μm) were cut and used for immunohistochemistry. To visualize the BDA, a tyramide signal amplification fluorescence system (Perkin Elmer, Waltham, MA, http://www.perkinelmer.com)> was used.

Visualization of Multisynaptic Neural Pathways

To visualize selective and functional transsynaptic neural pathways, wheat germ agglutinin (WGA)-expressing recombinant adenoviruses were used [24, 25]. Twelve weeks after injury, 1 μl of saline containing WGA-expressing virus at a titer of 1×10^{11} pfu/ml was injected into the bilateral motor cortices (0.5 μl per injection site). The injection site was 2.1 mm posterior to the bregma, 2 mm lateral to the bregma, and 0.7 mm in depth. Two weeks later, animals were perfused and the spinal cords were fixed as described above. Sections (15 μm) were cut and used for immunohistochemistry. Rabbit anti-WGA polyclonal antibody (3 μg/ml, Sigma) was preabsorbed with 1% acetone powder of mouse brains in blocking solution overnight at 4°C.

Ablation of Transplant-Derived Cells

Cell ablation experiments were performed as described previously [26, 27]. Diphtheria toxin (DT) was purified from conditioned medium of the PW8 strain of *Corynebacterium diphtheriae* by diethylaminoethyl Sepharose column chromatography and diluted to an appropriate concentration with saline. Seven weeks after injury, DT solution (50 μg/kg per day × 2 days) was administered by intraperitoneal injection into seven hiPS-NES cell-transplanted mice.

Statistical Analysis

We performed statistical analysis with an unpaired two-tailed Student's *t* test for single comparisons. For &&&BMS and BDA fiber analysis, we used repeated-measures ANOVA with Tukey-Kramer multiple comparison test at each point (Prism, GraphPad, LA Jolla, CA, http://www.graphpad.com). $p < .05$ was considered significant.

Results

Characterization of hiPS-Lt-NES Cells In Vitro

We have previously shown that hiPS-NES cells, which are reliably derived from different hiPS cell lines, exhibit consistent characteristics such as continuous expandability, stable neuronal and glial differentiation, and the capacity to generate functional mature human neurons [11]. hiPS-lt-NES cells can be expanded in the presence of FGF2 and EGF in monolayer culture, and express the NSC markers Sox2 and Nestin (Fig. 1A) and the radial glial marker BLBP (Supporting Information Fig. 1), but not the ES/iPS cell markers Oct3/4 or Nanog (not shown).

To visualize transplanted cells by both luminescence and fluorescence, hiPS-lt-NES cells were infected with lentiviruses engineered to express luciferase and GFP (Fig. 1B). Almost all hiPS-lt-NES cells were infected (Fig. 1C, middle), and we isolated only strongly GFP-expressing cells for use in subsequent in vitro and transplantation experiments (Fig. 1C, right).

We then examined whether lentiviral infection affected the differentiation potential of hiPS-lt-NES cells. Uninfected and infected hiPS-lt-NES cells were induced to differentiate by removal of growth factors and cultured in the presence of 1% FBS for 4 weeks. Both hiPS-lt-NES cell population differentiated into large and small numbers of Tuj1-positive neurons and GFAP-positive astrocytes, respectively, as observed in our previous study [11] (Fig. 1D). Quantitative analysis revealed no significant differences in the proportions of differentiated cells between uninfected and infected hiPS-lt-NES cells (Fig. 1E). Thus, we concluded that lentiviral infection did not influence the differentiation potential of hiPS-NES cells.

ID: ananda | Black Lining: [ON] | Time: 11:32 | Path: N:/3b2/STEM/Vol00000/120053/APPFile/JW-STEM120053

Transplantation of hiPS-Lt-NES Cells into the Injured Spinal Cord Improves Functional Recovery of Hind Limbs

In the present study, we used NOD-SCID mice, which are a suitable model for xenograft research because they are constitutively immunodeficient; their pathology and innate immune response after SCI are also similar to those of other mouse strains [4, 9, 28].

Previous studies have already shown that transplantation of human NSCs from fetal spinal cord or brain tissue improves locomotor functional recovery of SCI models [3, 4]. Nevertheless, only recently has the efficacy of hiPS-NSC transplantation into SCI begun to be investigated [9]. To determine whether our hiPS-lt-NES cells have a therapeutic capability, we first sought to compare the effects of these cells with those of human fetal spinal cord-derived NSCs (hsp-NSCs). Seventy-kilodyne contusive SCI was applied at the ninth thoracic vertebral level of mouse spinal cords, and 1 week later we injected medium alone (SCI control), or medium containing hsp-NSCs or hiPS-lt-NES cells, into the epicenter. We then monitored the animals' hind limb motor function using the BMS [19] for at least 8 weeks. All mice showed complete paralysis at 1-day after SCI (BMS scores were 0, Supporting Information Video 1). At 8 weeks after SCI, control mice could move their hind limbs but could not support their own weight (BMS scores were approximately 2, Supporting Information Video 2). In contrast, mice that received hsp-NSCs could touch the ground with their paws and/or support their body weight using their hind limbs (BMS scores were 3-4). The hiPS-lt-NES cell-transplanted group also showed functional recovery (BMS scores were 3-4, Supporting Information Video 3) compared to the control group, and there was no significant difference in BMS scores between the hsp-NSC- and hiPS-lt-NES cell-transplanted
F2 groups (Fig. 2A). These results indicate that hiPS-NES cells have a comparable therapeutic effect to hsp-NSCs on SCI.

Next, to evaluate the recovery of descending pathways from the motor cortex to the hind limb motor neurons, we monitored MEPs at 12 weeks after SCI. We stimulated motor cortices electrically and recorded MEP amplitudes from the hamstring muscles. The MEP amplitudes in the hiPS-NES cell-transplanted group were significantly higher than those in the SCI control group (Fig. 2B, 2C). Furthermore, the latency of MEP response in the hiPS-lt-NES cell-transplanted group was significantly shorter than that in the SCI control group (Fig. 2D). These results suggest that transplantation of hiPS-lt-NES cells into the injured spinal cord stimulates the functional recovery of hind limbs.

Transplanted hiPS-Lt-NES Cells Survive and Differentiate in the Injured Spinal Cord of NOD-SCID Mice

We have established hiPS-lt-NES cells that express luciferase and GFP, enabling us to trace the survival of the transplanted cells with a bioluminescence imaging system which detects photon signals from living cells after administration of luciferin (a substrate of luciferase) to the mice [18]. The photon
F3 signals decreased gradually after transplantation (Fig. 3A) and approximately 20% of transplanted hiPS-lt-NES cells survived in the injured spinal cord at 5 weeks after SCI (4 weeks after transplantation), whereafter the photon signals remained stable (Fig. 3B).

Using immunohistochemistry, we found that GFP-positive transplanted cells survived and migrated to both rostral and caudal areas around the lesion site in the injured spinal cord (Fig. 3C). High-magnification images showed that transplanted hiPS-lt-NES cells extended processes into both gray and white matter (Fig. 3C-1, 3C-2).

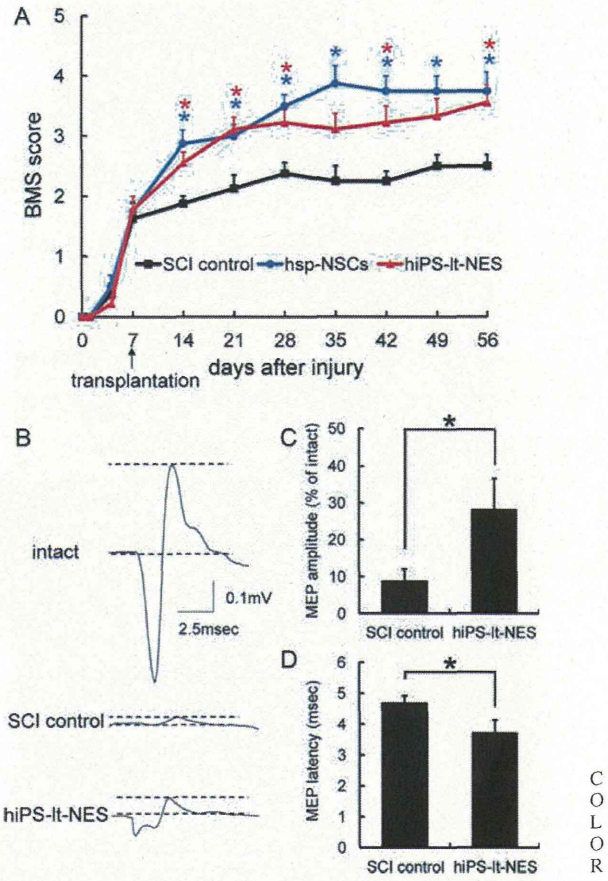

Figure 2. Transplantation of hiPS-lt-NES cells into the injured spinal cord improves functional recovery of hind limbs. **(A):** Time course of functional recovery of hind limbs after SCI. Data are means ± SEM (SCI control, $n = 8$; hsp-NSCs, $n = 8$; hiPS-lt-NES cells, $n = 9$). Mean BMS values of hsp-NSC- and hiPS-lt-NES cell-transplanted groups were compared with those of the SCI control group. *, $p < .05$. There was no significant difference between values in the hsp-NSC group and the hiPS-lt-NES cell group. **(B):** Representative MEP waves of intact, SCI control, and hiPS-lt-NES cell-treated mice at 12 weeks after injury. The motor cortices were stimulated and MEP amplitudes were recorded from hamstring muscles. Amplitudes from onset to peak of the negative deflection were measured. **(C):** Relative values of the mean MEP amplitudes. Values are expressed as percentages of those in intact mice. Mean relative MEP amplitude in the hiPS-lt-NES cell group was significantly higher than that in the SCI control group. *, $p < .05$. Data are means ± SD ($n = 3$). **(D):** Relative values of the mean MEP latency. Mean relative MEP latency in the hiPS-lt-NES cell group was significantly shorter than that in the SCI control group. *, $p < .05$. Data are means ± SD ($n = 3$). Abbreviations: BMS, Basso Mouse Scale; hiPS-lt-NES, human induced pluripotent stem cell-derived long-term self-renewing neuroepithelial-like stem; MEP, motor-evoked potential; hsp-NSC, human fetal spinal cord-derived neural stem cell; and SCI, spinal cord injury.

We then examined the differentiation of the transplanted hiPS-lt-NES cells in the injured spinal cord and found a similar differentiation tendency to that observed in vitro (Fig. 1D, 1E), with many GFP-positive transplant-derived cells having become Tuj1-positive neurons (75%) at 8 weeks after SCI (Fig. 3D–3F). Twenty percent of GFP-positive transplanted cells differentiated into GFAP-positive astrocytes, while their

J_ID: STEM Customer A_ID: STEM1083 Date: 16-March-12 Stage: Page: 6

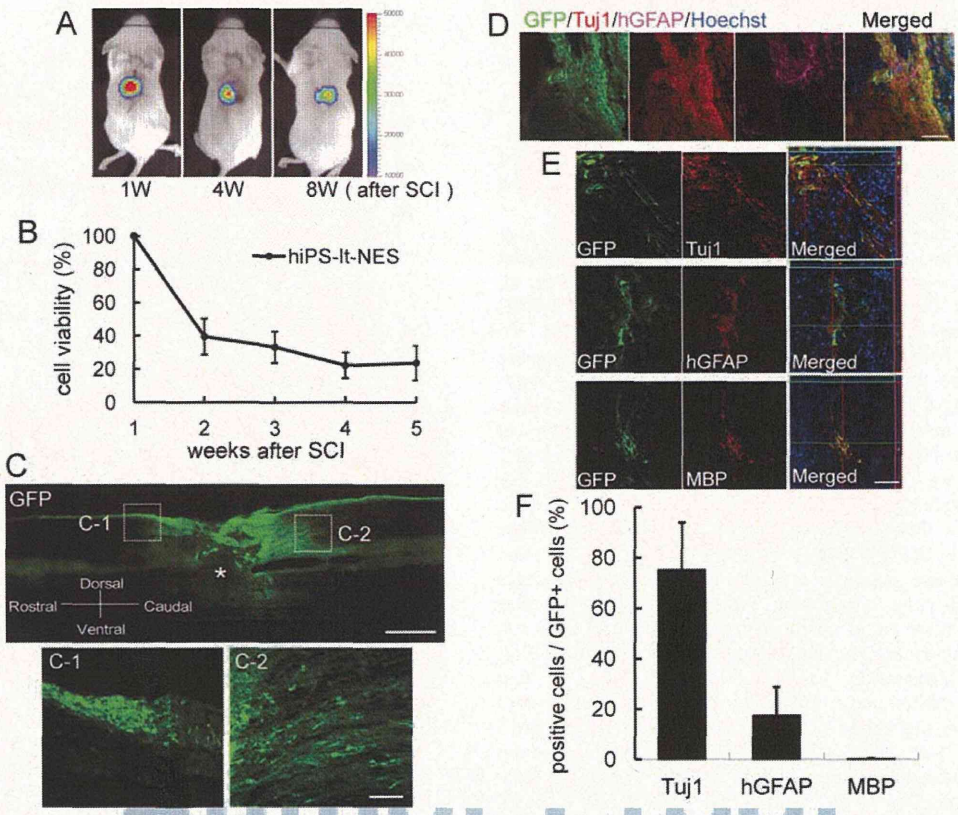

COLOR

Figure 3. *Transplanted human induced pluripotent stem cell-derived long-term self-renewing neuroepithelial-like stem (hiPS-lt-NES) cells survive and differentiate in the injured spinal cord of nonobese diabetic-severe combined immunodeficient mice.* **(A):** Survival of transplanted cells was checked every week using a bioluminescence imaging system; left, 2 hours after transplantation; middle, 4 weeks after SCI; and right, 8 weeks after SCI. **(B):** Time course of transplanted hiPS-lt-NES cell survival in SCI model mice. Optical signal intensity was measured using the bioluminescence imaging system. Quantification of the photon intensity revealed that approximately 20% of the transplanted cells survived 5 weeks after SCI; thereafter, the photon signals remained stable. Data are means ± SEM ($n = 6$). **(C):** Sagittal sections of SCI model mice treated with hiPS-lt-NES cells at 8 weeks after transplantation. Sections were stained with anti-GFP antibody (green). The epicenter of the SCI is indicated (*). Higher-magnification images of the white dotted boxes (C-1 and C-2) show GFP-positive transplant-derived cells extending their processes into gray and white matter. **(D):** Immunostaining images, 8 weeks after injury, of hiPS-lt-NES cells grafted into spinal cord. Spinal cord sections were stained with anti-GFP (green), hGFAP (magenta) and Tuj1 (red) antibodies and with Hoechst (blue). **(E):** Confocal images, 8 weeks after injury, of hiPS-lt-NES cells transplanted into spinal cord, revealing transplanted cells which were double-positive for GFP and markers of neural lineages. **(F):** Quantitative analyses of Tuj1-positive neurons, hGFAP-positive astrocytes, and MBP-positive oligodendrocytes as in E. Data are means ± SD ($n = 3$). Scale bars = 500 μm in C, 100 μm in C-1, C-2, D, and E. Abbreviations: GFP, green fluorescent protein; hGFAP, anti-human-specific glial fibrillary acidic protein; MBP, • • •; and SCI, spinal cord injury.

AQ6

differentiation into MBP- or APC-positive oligodendrocytes was less than 1% (Fig. 3E, 3F, Supporting Information Fig. 2). These data indicate that transplanted hiPS-lt-NES cells differentiate preferentially into neurons in the injured spinal cord.

hiPS-Lt-NES Cell Transplantation Does Not Promote CST Axon Re-Extension After SCI

Since transplanted NSCs have been reported to play a supportive role in the re-extension of injured axons [29], we examined the effect of the transplanted hiPS-lt-NES cells on CST first-order axonal regeneration. We injected BDA into the bilateral motor cortices and labeled CST first-order neuron axons by anterograde tracing [21, 22]. Because BDA is not transported from first- to second-order neurons across the synapse, only the axons of first-order neurons in the CST are visualized by this method.

In the region caudal to the injury site, >50% of the labeled fibers observed at 5 mm anterior to the lesion site were detected in the intact mice, whereas almost no BDA-traced CST fibers could be seen in the SCI control or hiPS-lt-NES cell-transplanted mice (Fig. 4A). Quantitative analysis revealed that there was no significant difference in the number of BDA-labeled fibers between the SCI control and hiPS-lt-NES cell-treated groups at any position up to 5 mm on either side of the lesion site (Fig. 4B). Although we cannot exclude possibilities such as the re-extension of descending raphespinal axons, which are also important for the motor functional recovery of hind limbs [30, 31], these results suggest that the regeneration of CST axons, if it occurs, cannot be a major contributing factor in the recovery induced by hiPS-lt-NES cell transplantation in our SCI model.

F4

Local Neurons Reconstruct Disrupted CST Neuronal Circuits in a Relay Manner

Recent studies have revealed that local endogenous and transplant-derived neurons can form new neuronal circuits and make synaptic connections after SCI [32–34]. To determine

ID: ananda | Black Lining: [ON] | Time: 11:32 | Path: N:/3b2/STEM/Vol00000/120053/APPFile/JW-STEM120053

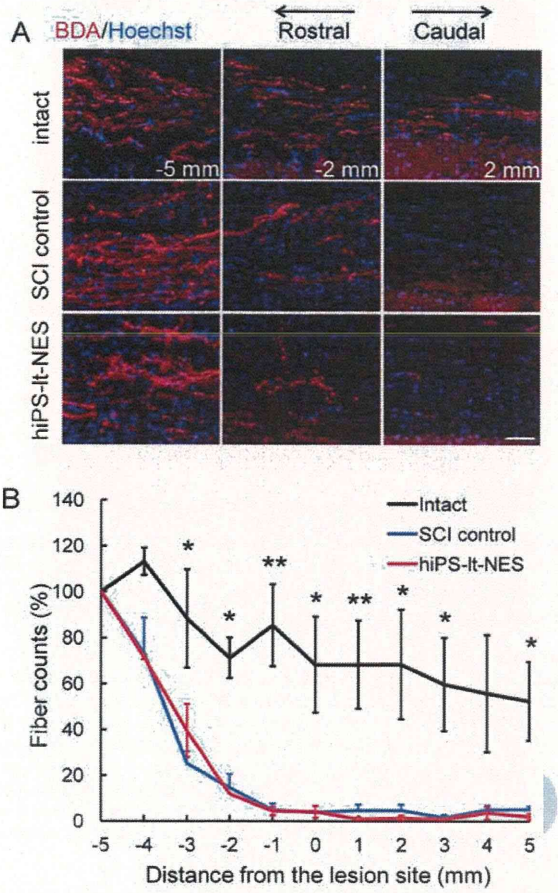

Figure 4. hiPS-lt-NES cell transplantation does not promote corticospinal tract (CST) axon re-extension after SCI. **(A):** Representative pictures of BDA-labeled CST fibers (red) at 5 and 2 mm rostral and 2 mm caudal to the lesion site at 12 weeks after SCI. Hoechst (blue) shows nuclear staining. Scale bar = 50 μm. **(B):** Quantification of the labeled CST fibers in the spinal cords of untreated, SCI control, and hiPS-lt-NES cell-transplanted mice. The x-axis indicates specific locations along the rostro-caudal axis of the spinal cord, and the y-axis indicates the ratio of the mean number of BDA-labeled fibers at the indicated site to that at 5 mm rostral to the lesion site (thoracic vertebra [Th] 9). Intact mice were compared with SCI control mice. *, $p < .05$; **, $p < .01$. There was no significant difference in the number of BDA-labeled fibers between hiPS-lt-NES cell-treated (blue line) and SCI control groups (red line). Data are means ± SEM ($n = 5$). Abbreviations: BDA, biotinylated dextran amine; hiPS-lt-NES, human induced pluripotent stem cell-derived long-term self-renewing neuroepithelial-like stem; and SCI, spinal cord injury.

COLOR

whether disrupted CSTs were reconstructed by forming a local neuronal relay, we injected WGA-expressing adenoviruses into the motor cortex of the hind limb area at 12 weeks after SCI. WGA, a plant lectin, has been widely used as a tracer of neuronal pathways [24, 25] because it is transported in axons and dendrites, and across synapses, to second- and even third-order neurons.

After injection, we could detect WGA-immunoreactive intracellular granule-like structures in MAP2ab-positive neurons (Fig. 5A). Furthermore, we found that hiPS-lt-NES cell-treated mice had more WGA/Map2ab double-positive cells than SCI control mice in the caudal region below the injured site (Fig. 5A, 5B). Taking these data and the results of the BDA experiment into consideration, it is suggested that WGA was transferred to the caudal area through the lesion site via new synaptic connections, and that hiPS-lt-NES cell transplantation promoted the CST reconstruction without CST axonal re-extension. In support of this proposition, we could observe GFP-positive transplant-derived neurons adjacent to synaptophysin-positive patches (Fig. 5C-1 and 5C-1′). Furthermore, immunohistochemistry using species-specific antibodies for presynaptic markers revealed that transplant-derived neurons made synapses with endogenous neurons, suggesting that they reconstructed disrupted CST neuronal circuits in a relay fashion (Fig. 5C-2, 5C-2′, 5C-3, and 5C-3′).

hiPS-Lt-NES Cell Transplantation Promotes the Survival of Endogenous Neurons

Massive endogenous cell death is observed in the injured spinal cord, probably due to environmental changes such as increased levels of inflammatory cytokines [35, 36]. Previous studies have suggested that neurotrophic factors secreted from transplanted cells could alleviate cell death and thereby contribute to improved locomotor function after SCI [37]. We therefore wanted to examine whether transplanted hiPS-lt-NES cells influence the survival of endogenous neurons. We performed immunohistochemistry and counted the number of NeuN-positive/GFP-negative endogenous neurons around the lesion site (Fig. 6A) and found that the number of endogenous neurons in the hiPS-lt-NES cell-treated mice was significantly higher than that in the SCI control (Fig. 6B). These findings indicate that transplantation of hiPS-lt-NES cells alters the environment of the injured spinal cord and promotes the survival of endogenous neurons.

Transplanted Cells Contribute Directly to Functional Recovery of Hind Limb Movement in SCI Model Mice

Ablation of specific cells is a useful method to evaluate their functional contribution in animal models. Mouse and rat cells are less sensitive to DT than human cells, which express human heparin-binding epidermal growth factor-like growth factor (hHB-EGF) as a DT receptor [26, 27]. We administered DT to hiPS-lt-NES cell-transplanted mice at 7 weeks after SCI. Using an in vivo imaging system, we were able to trace the survival of transplanted cells while evaluating hind limb function. Almost all the transplanted hiPS-lt-NES cells were specifically ablated following DT administration (Fig. 7A). After ablation of the transplanted cells, the BMS score of hiPS-lt-NES cell-treated mice dropped to a level similar to that of SCI control mice, although the reduction was not large enough to make the score differ significantly from that attained by hiPS-lt-NES cell-treated mice without DT administration (Fig. 7B). This may be because transplanted hiPS-lt-NES cells promoted the survival of endogenous neurons (Fig. 6) that participated in the reconstruction of disrupted neuronal circuitry. Nevertheless, these results suggest that transplanted hiPS-lt-NES cells play direct and important roles in the functional recovery of the injured spinal cord.

Discussion

The advent of cell reprogramming and the establishment of iPS cells have provided new prospects for stem cell transplantation therapy [7, 8], and a large number of different types of iPSCs have already been generated by various methods [38–40]. Transplantation of NSCs into the injured spinal cord has been shown to be effective, and with recent advances in stem cell biology, particularly in human ES/iPS cells, we anticipate

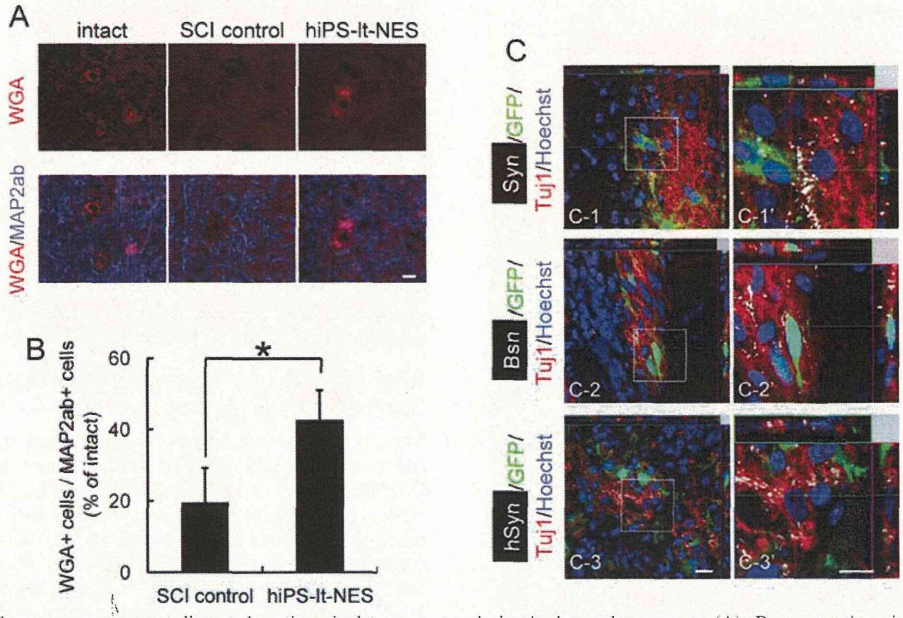

COLOR

Figure 5. Local neurons reconstruct disrupted corticospinal tract neuronal circuits in a relay manner. **(A):** Representative pictures of WGA-labeled neuronal cell bodies located in the caudal area (Th11 to lumbar vertebra [L] 1) at 12 weeks after spinal cord injury (SCI; left, intact mice; middle, SCI control mice; and right, hiPS-lt-NES cell-treated mice). Spinal cord sections were stained with anti-WGA (red) and anti-MAP2ab (neuronal marker, blue) antibodies. WGA immunoreactivity was observed as intracellular granule-like structures. **(B):** WGA-positive cells/MAP2ab-positive neurons in the caudal area were quantified. Values are expressed as percentages of those in intact mice. The percentage of WGA-positive cells in hiPS-lt-NES cell-treated mice was significantly higher than that in SCI control mice. *, $p < .05$. Data are means ± SD ($n = 3$). **(C):** Spinal cord sections were stained with anti-GFP and Tuj1 antibodies, Hoechst (blue), and Syn, Bsn, or hSyn antibodies. (C-1) Representative confocal image showing that GFP (green) and Tuj1 (red) double-positive transplant-derived neurons were adjacent to synaptophysin-positive patches (white). (C-1′) High-magnification view of boxed area in (C-1). (C-2) Host and graft synapses were distinguished using a monoclonal antibody for the presynaptic marker Bsn that selectively recognizes rat and mouse, but not human, epitopes. Confocal image showing that GFP (green) and Tuj1 (red) double-positive transplant-derived neurons were in contact with Bsn-positive host synapses (white). (C-2′) High-magnification view of boxed area in (C-2). (C-3) Confocal images showing that GFP (green)-negative and Tuj1 (red)-positive endogenous neurons were in contact with hSyn-positive synapses (white). (C-3′) High-magnification view of boxed area in (C-3). Scale bars = 10 μm. Abbreviations: Bsn, anti-Bassoon; GFP, green fluorescent protein; hiPS-lt-NES, human induced pluripotent stem cell-derived long-term self-renewing neuroepithelial-like stem; hSyn, anti-human-specific synaptophysin; Syn, anti-synaptophysin; and WGA, wheat germ agglutinin.

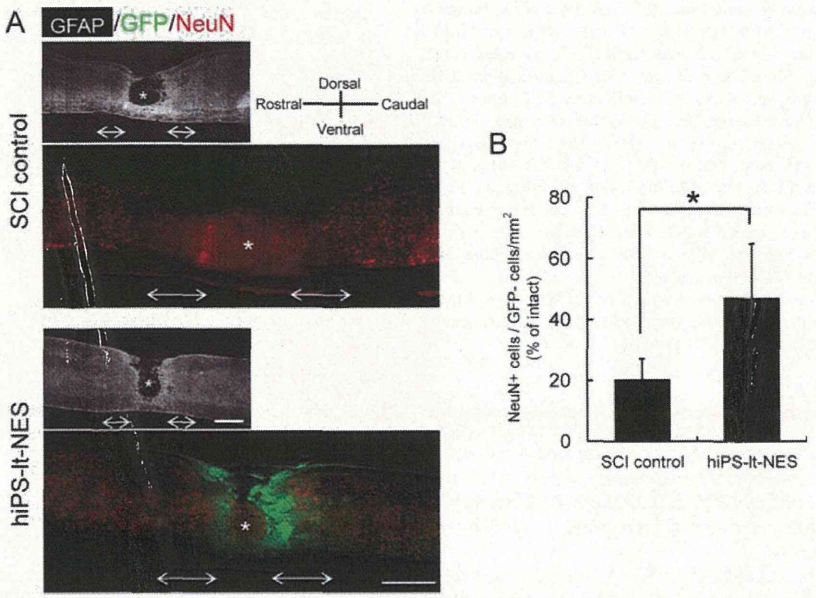

COLOR

Figure 6. Transplanted hiPS-lt-NES cells promote the survival of endogenous neurons. **(A):** Representative sagittal sections of SCI control and hiPS-lt-NES cell-transplanted mice at 12 weeks after SCI. Sections were stained with anti-GFAP (white), anti-NeuN (mature neuronal marker, red) and anti-GFP (green) antibodies. Two 500-μm regions, at the rostral and caudal edge of the lesioned site (double-headed arrows), were selected for the assessment. The epicenter of the SCI is indicated (*). Scale bars = 500 μm. **(B):** Quantification of NeuN-positive/GFP-negative endogenous neurons. Values are expressed as percentages of those in intact mice. The number of NeuN-positive/GFP-negative endogenous neurons in hiPS-lt-NES-treated mice was significantly higher than that in SCI control mice. *, $p < .05$. Data are means ± SD ($n = 3$). Abbreviations: GFAP, glial fibrillary acidic protein; GFP, green fluorescent protein; hiPS-lt-NES, human induced pluripotent stem cell-derived long-term self-renewing neuroepithelial-like stem; and SCI, spinal cord injury.